

Using Electrophysiology and *In Silico* Three-Dimensional Modeling to Reduce Human *Ether-a-Go-Go*-Related Gene K⁺ Channel Inhibition in a Histamine H3 Receptor Antagonist Program

Adam J. Davenport,¹ Clemens Möller,² Alexander Heifetz,¹ Michael P. Mazanetz,¹ Richard J. Law,¹ Andreas Ebnetz,² and Mark J. Gemkow²

¹Evotec Ltd., Milton Park, Abingdon, United Kingdom.

²Evotec AG, Hamburg, Germany.

ABSTRACT

The histamine H3 receptor (H3R) plays a regulatory role in the presynaptic release of histamine and several other neurotransmitters, and thus, it is an attractive target for central nervous system indications including cognitive disorders, narcolepsy, attention-deficit hyperactivity disorder, and pain. The development of H3R antagonists was complicated by the similarities between the pharmacophores of H3R and human ether-a-go-go-related gene (hERG) channel blockers, a fact that probably prevented promising compounds from being progressed into the clinic. Using a three-dimensional *in silico* modeling approach complemented with automated and manual patch clamping, we were able to separate these two pharmacophores and to develop highly potent H3R antagonists with reduced risk of hERG liabilities from initial hit series with low selectivity identified in a high-throughput screening campaign.

INTRODUCTION

The histamine H3 receptor (H3R) is a G protein-coupled receptor and one of four receptors of the histamine receptor family, which was identified by J.C. Schwartz's group in 1983 and characterized as a presynaptic autoreceptor that controls the release of histamine.¹ A few years later the H3R was also characterized as a heteroreceptor on nonhistaminergic neurons being capable of regulating the release of many other important neurotransmitters, including acetylcholine, norepinephrine, dopamine, and serotonin.^{2–5} The H3R is expressed predominantly in the central nervous system, in regions that have been associated with cognition (cortex and hippocampus), sleep, and homeostatic regulation (hypothalamus), as well as in regions involved in nociception (e.g., specific thalamic areas, dorsal root ganglia, and spinal cord).^{6–8} Given its widespread distribution and

its ability to affect multiple neurotransmitter systems, modulation of H3R activity has been proposed for a broad range of indications including Alzheimer's disease, attention-deficit hyperactivity disorder, sleep disorders, pain, and obesity.⁹

Early clinical H3R antagonists/inverse agonists were imidazole-containing compounds such as Gliatech's clinical candidate GT-2331 (Cipralisant, Perceptin®).^{10,11} Imidazole-containing compounds bare the inherent risk of cytochrome P450 isoenzyme inhibition and consequential drug–drug interactions. It is possible that these drug–drug interactions might have contributed to termination of their clinical development. More recently, pharmaceutical and biotechnology industries have focused efforts on development of nonimidazole H3R antagonists.^{11–13} Although the majority of nonimidazole H3R antagonist classes appear not to significantly inhibit the cytochrome P450 family of enzymes, many H3R antagonist programs have demonstrated the potential for phospholipidosis.^{14,15} Other compounds have wrestled with binding to P-gp transporters (P-glycoprotein) or, even more importantly, have suffered from significant blockade of the human ether-a-go-go-related gene (hERG) K⁺ channel.^{14,16–18}

Blockade of the hERG channel can delay cardiac repolarization and thereby prolong cardiac action potential duration. This predisposes affected individuals to a life-threatening arrhythmia called Torsades de pointes. This discovery forced pharmaceutical companies to withdraw several drugs with hERG channel liabilities from the market, and drug regulatory agencies now request testing of drug candidates for inhibition of the hERG channel activity before entry into humans. Consequently, it became routine practice in the pharmaceutical industry to profile compounds against the hERG channel early in the drug-development process.

Compounds that inhibit the H3R with high affinity contain a basic amine linked to an aromatic or general lipophilic region that is connected to either (1) a second basic site, (2) a polar group, (3) a lipophilic region, or (4) an acidic group,^{12,19–21} resulting in pharmacophores that comprise significant similarity to the predicted pharmacophore for hERG blockers (Fig. 1).²² As an example, Abbott's preclinical candidate ABT-239 (Table 1) is reported to exhibit strong binding to the hERG K⁺ channel (K_i = 0.45 nM; 420-fold

ABBREVIATIONS: ESPC, electrostatic potential complementarity; hERG, human ether-a-go-go-related gene; H3R, histamine H3 receptor; MOE, molecular operating environment; MPC, manual patch-clamp; QSAR, quantitative structure activity relationship; 3D, three dimensional.

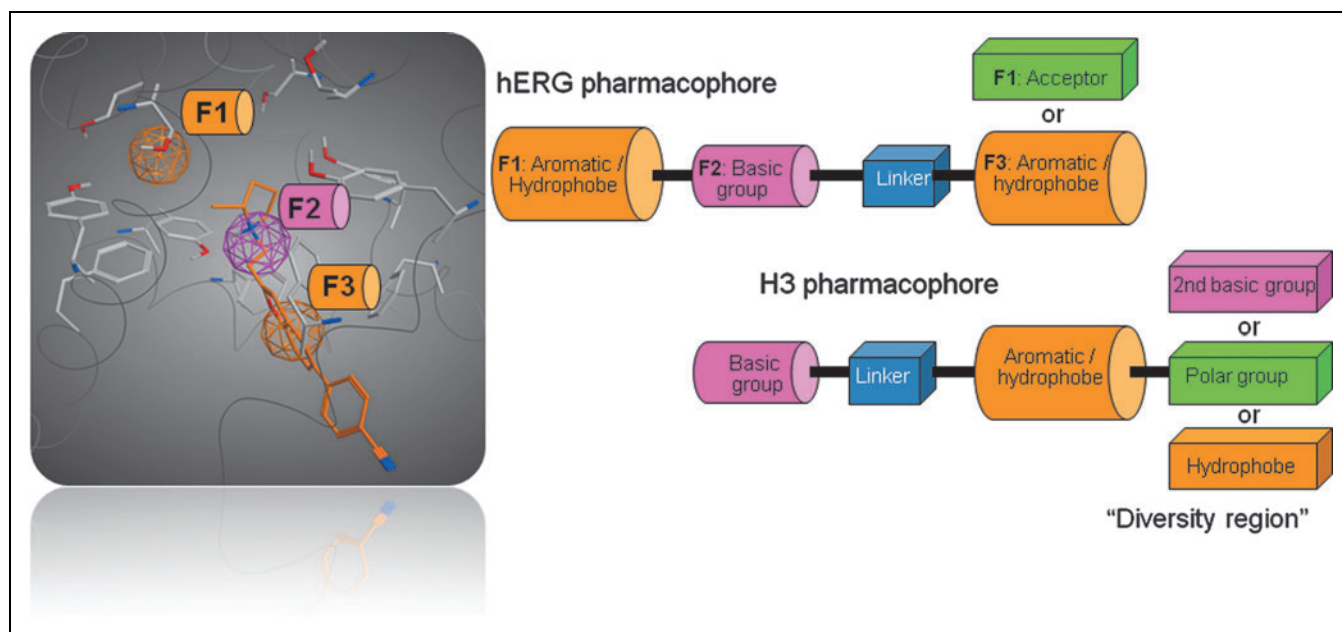


Fig. 1. Comparison of the hERG and H3R pharmacophore models for nonimidazole H3R antagonists shown on the right. On the left, ABT-239 is docked into the hERG pore to show where the three main pharmacophore points are located. hERG, human *ether-a-go-go*-related gene channel; H3R, histamine H3 receptor.

selectivity H3R/hERG), which manifests itself in a dose-dependent QTc prolongation in dog (Altenbach, personal communication) and monkey.¹⁸

The obvious goal of a H3R drug discovery program, therefore, is to design molecules that have high inhibitory affinity for the H3R but not for the hERG channel. But changing/removal of a whole pharmacophore point from a molecule series is likely to dramatically affect its on-target activity, especially in the case of H3R, where the target and hERG pharmacophore maps are so similar. In this article, we present the successful use of a combined approach of *in silico* three-dimensional (3D) modeling together with manual patch-clamp (MPC) and automated patch-clamp techniques, to achieve the goal of designing highly potent H3R antagonists with low risk of hERG channel blockade. That is, the hERG channel *in silico* modeling in support of the H3R project is aimed to address two points: first, to provide a structural explanation and prediction of the hERG potency of the H3R antagonists, and second, to suggest a strategy for how to diminish hERG liability via small changes to the lead compounds.

To this end we developed a novel three-tiered hierarchical algorithmic protocol, which progressively becomes more complex with successive tiers. The simplest is the pharmacophore-guided docking of the molecules into the hERG homology model. The second layer is the evaluation of the interactions between the hERG protein and a ligand with 3D quantitative structure–activity relationship (QSAR) models.²³ The level of complexity employed is dependent upon the ability of the model to rationalize the observed hERG activity. The third tier is the calculation of complementarities between the electrostatic potentials of the hERG protein and a ligand, and the mapping of the associated attractive and repulsive interactions onto the

surface of the ligand. This information is also used in guiding small chemical changes to be made to known hERG actives.

MATERIALS AND METHODS

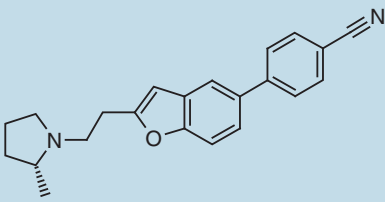
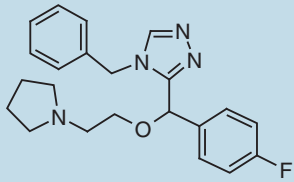
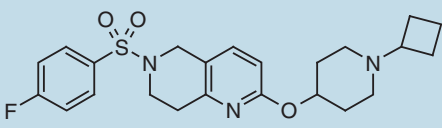
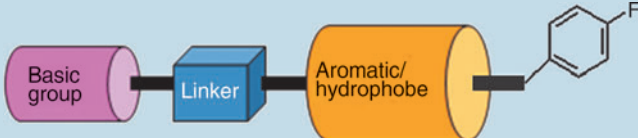
In Silico Work

Pharmacophore-driven docking into the hERG channel homology model. The hERG model was generated and optimized using the homology modeling module as implemented in the Chemical Computing Group's Molecular Operating Environment (MOE) package,³⁹ starting with the crystal structure of the bacterial potassium channel, KvAP (from the archaeobacterium *Aeropyrum pernix*), as a template (Protein Database Identifier: 1ORQ).²⁵

The three-feature hERG pharmacophore model was derived from a training set of 37 compounds compiled from both the literature and in-house sources.²⁶ Only compounds with two or more reported experimental measurements within a range of one log-order were included. Two pharmacophore features (F1 and F3) require aromatic moieties, which would interact with neighboring Tyr or Phe residues. The third pharmacophore feature (F2) is a cationic (basic) nitrogen or hydrogen bond donor group, which interacts with the neighboring Tyr residues. The pharmacophore model is satisfied when a ligand interacts with F2 in addition to F1 and/or F3 (Fig. 1).

2D hERG models. Two 2D hERG QSAR models were built to deal with discrepancies in published hERG channel inhibition data. Model 1 favors accuracy in that it uses a training set of 36 compounds (see *Supplementary Tables S1 and S2*; *Supplementary Data* are available online at www.liebertonline.com/adt) for which

Table 1. Human Histamine H3 Receptor and Human *Ether-a-Go-Go*-Related Gene K⁺ Channel Activities of Evotec Early Lead Compounds and ABT-239, Abbott's Earlier Preclinical Candidate

Compound	Structure	Human H3R IC ₅₀ (nM) ^a	MPC hERG IC ₅₀ (nM) ^b
ABT-239		1.5	290
1a		1,071	3,800
1b		2.5	680
1c ^c		0.3	990

See Ref. 33 for complete details of human H3R assay conditions.

^aValues are arithmetic means of two or more experiments; individual values do not differ more than threefold from the mean.

^cCompound 1c is shown as an acronym for intellectual property reasons and was the early lead that led to the molecules depicted in Table 2. hERG, human *ether-a-go-go*-related gene; H3R, histamine H3 receptor; MPC, manual patch-clamp.

published data are within one order of magnitude. Model 2 favors diversity (*Supplementary Fig. S1*) and uses a set of 90 compounds for which, in many cases, only a single data point exists. The models had r^2 of 0.84 and 0.7 and covered 53 and 54 descriptors, respectively, and a log IC₅₀ (μM) range from 4 to -3. The non-cross-validated variance coefficient (r^2) and the cross-validated variance coefficient (q^2) were used to describe how well a model can reproduce the data under analysis and the internal consistency of the model. Cross-validation was performed by dividing the training sets into seven groups and developing a number of parallel models for the data devoid of one group. The omitted group then became the test set for the reduced model and residuals for the test sets were calculated. A measure of the predictivity of the models, termed predictive residual sum of squares, was derived from the sum of

squares of these differences for all parallel models. The q^2 value that resulted in the optimum number of components and lowest predictive residual sum of squares was used. The Y variables were mean-centered and scaled to unit variance.

Mapping electrostatic potential complementarity. Calculation of the electrostatic potential complementarity (ESPC) between a ligand and the hERG protein model allows for the recognition of key interaction points that appear to be sensitive to small structural changes of the ligand.²⁷ We developed a method to calculate the ESPC, which provides a sum total of the electrostatic interactions between the hERG protein and a ligand and also details of specific positions where attractive and repulsive interactions occur on the ligand surface. The results of this calculation can be represented visually.²⁸ In addition,

the method was developed to compensate for small ligands and sidechain positional errors caused by the use of an hERG homology model and the sensitivity of docking procedures. The EPCS is calculated as follows (Equation 1)²⁹:

$$\text{EPCS} = \sum_{i=1}^N \sum_{j=1}^N \sum_{k=1}^N E_{i,j,k}^{\text{hERG}} \times E_{i,j,k}^{\text{ligand}} \quad (1)$$

where $E_{i,j,k}^{\text{hERG}}$ and $E_{i,j,k}^{\text{ligand}}$ are electrostatic descriptors derived from the calculated electrostatic potentials $P_{i,j,k}^{\text{hERG}}$ and $P_{i,j,k}^{\text{ligand}}$ of the hERG protein and a ligand, respectively, at the grid point (i, j, k) .^{30,31} To visualize the zones where the ligand is attracted to or repulsed from hERG, Leonard-Jones particles were created at each grid point, that contributes significantly (above a defined threshold) to the EPCS and are mapped to the ligand surface. The threshold for defining significant interactions was set by ranking the grid points according to the strength of their interaction and then taking the top 20% of this ranking list.

In Vitro Work

Molecular biology. The cDNA coding the hERG product (hERG; GenBank accession no.: U04270) was cloned into the pcDNA3 vector (Invitrogen). A C-terminal myc-tag was introduced via PCR. Plasmids were introduced into Chinese hamster ovary cells using the transfection reagent liposome formulation of the cationic lipid 1,2-dimyristyloxypropyl-3-dimethyl-hydroxy ethyl ammonium bromide-chloesterol (DMRIE-C), according to the manufacturer's instructions (Invitrogen; catalog no.: 10459-014). Stably transfected cells were selected in the presence of 800 $\mu\text{g}/\text{mL}$ G-418 (Invitrogen) and 5 $\mu\text{g}/\text{mL}$ blasticidin (Invitrogen) and clonal cell lines were established. Expression of protein was analyzed by means of immunofluorescence using antibodies directed against the epitope tag. The functional expression of the ion channels was validated by electrophysiological measurements.

Cell culture. Cells were grown at 37°C and 5% CO₂ in modified Eagle's medium- α (Invitrogen) supplemented with 10% (v/v) heat-inactivated fetal calf serum, 1% (v/v) penicillin/streptomycin/glutamate solution (Invitrogen; catalog no.: 10378-016), and 850 $\mu\text{g}/\text{mL}$ G-418 supplemented with 110 mM HEPES [pH 7.4].

Electrophysiology and Data Analysis

General procedure. Patch-clamp experiments were performed in the voltage-clamp mode³² and whole-cell currents were recorded using manual pipette-based patch-clamp as well as automated and semiautomated planar chip-based patch-clamp electrophysiology.

Manual (pipette-based) patch-clamp electrophysiology. Extracellular solutions for MPC electrophysiology contained 130 mM NaCl, 5.4 mM KCl, 1.8 mM CaCl₂, 1 mM MgCl₂, 5 mM glucose, and 10 mM HEPES adjusted to pH 7.4; intracellular solutions contained 130 mM

KCl, 1 mM MgCl₂, 5 mM glucose, 1 mM EGTA, 2 mM MgATP, and 10 mM HEPES adjusted to pH 7.2. Patch pipettes were pulled (puller from Science Products GmbH, Hofheim, Germany) from borosilicate glass tubes (GC 150; Clark Electromedical Instruments, Pangbourne, UK). Current signals were amplified and digitized by an EPC 9 patch-clamp amplifier (HEKA Electronics, Lambrecht, Germany), stored, and analyzed on a personal computer using the Pulse/Pulsefit software (HEKA Electronics). Experiments were conducted at room temperature (21°C \pm 2°C).

Planar patch-clamp electrophysiology. Experiments were performed on two different planar patch-clamp electrophysiology devices, the automated PatchLiner 8 (Nanion Technologies GmbH, Munich, Germany) using 16-well planar chips (catalog no.: NPC-16_Med) and the semiautomated Port-a-Patch (Nanion Technologies GmbH) using single-cell planar chips. Extracellular solutions for planar patch-clamp electrophysiology contained 160 mM NaCl, 4.5 mM KCl, 2 mM CaCl₂, 1 mM MgCl₂, 5 mM glucose, and 10 mM HEPES adjusted to pH 7.4; intracellular solutions contained 10 mM KCl, 135 mM KF, 10 mM NaCl, 2 mM MgCl₂, 5 mM glucose, 10 mM EGTA, and 10 mM HEPES adjusted to pH 7.2. Current signals were amplified and digitized by EPC 10 double patch-clamp amplifiers (HEKA Electronics), stored, and analyzed on a personal computer using the Pulse/Pulsefit software (HEKA Electronics). The experiments were controlled by the PatchControl software (Nanion Technologies GmbH). Experiments were conducted at room temperature (21°C \pm 2°C).

Stimulation protocol for the hERG-mediated current. In MPC experiments, cells were briefly characterized under control conditions by recording current-voltage relationships using the following stimulation protocol: Cells were held at -80 mV, depolarized to +20 mV for 1 s, and repolarized in steps from -120 mV to +40 mV in 10 mV intervals for 1 s each. Stimulation frequency was 0.1 Hz.

For investigating compound effects and reversibility of compound effects, cells were held at -80 mV and were depolarized for 1 s to +20 mV, followed by a 1 s partial repolarization back to -40 mV. Tail outward current amplitudes at -40 mV were analyzed. Currents were leak-current corrected. Stimulation frequency was 0.1 Hz.

In automated patch-clamp experiments, cells were clamped at a holding potential of -80 mV, depolarized to +40 mV for 500 ms, followed by a 500 ms partial repolarization to -40 mV. Currents were leak-current corrected. Stimulation frequency was 0.05 Hz.

Compound application and data evaluation. The compounds were dissolved in 100% dimethyl sulfoxide at required stock concentration; final dimethyl sulfoxide concentrations in the test solutions did not exceed 1%. The late tail outward current was measured for each partial repolarization, and compound effects were evaluated when a steady state of compound effects was reached. Reversibility of compound effects was evaluated after 5 min of withdrawal of the compounds.

Endogenous rundown of potassium currents was corrected by calculating an extrapolated time course under vehicle conditions using a biexponential fit of the equation $Y = a \times \exp(-ct) + b \times$

$\exp(-dx)$ to initially control stimuli. Experiments with a current rundown of more than 5% within the initial period were not included in the data analysis. Average current rundown was calculated to be $2.3\% \pm 1.9\%$ in 5 min.

An estimated concentration–response relation was calculated by nonlinear least-squares fits of the equation $f = 1/(1 + (C/IC_{50})^{nH})$ to the individual data points. The Hill coefficient (nH) and the half-maximal inhibiting concentration (IC_{50}) were calculated by the fitting routine.

RESULTS AND DISCUSSION

Identification of hERG Liabilities During Early Phases of Hit Expansion

A high-throughput screen of Evotec's screening collection (>250,000 compounds) was performed, resulting in the identification of several H3R hit compound clusters. Because of the propensity for H3R antagonists to block the hERG channel, we prioritized the hERG testing of key compounds during the hit expansion phase of the hit-to-lead work by means of MPC. Indeed, it became apparent that compounds from several interesting hit clusters showed inhibition of the hERG channel. *Table 1* illustrates Evotec H2L example compounds (1a–1c) along with Abbott's discarded preclinical candidate ABT-239, showing that hERG channel blockade assessment was advisable early in this drug discovery program (for details of the H3R assay conditions see Ref. 33). For compound 1c, only the relevant R group is shown for intellectual property reasons. Most of the compounds analyzed shared the common H3R pharmacophore (*Fig. 1*).

Although MPC is considered to be the method of choice for determination of hERG inhibition, it became apparent that a higher-throughput instrumental setup would be beneficial for the program. Hence, we established a new approach by combining a medium-throughput device, namely the Patchliner from Nanion Technologies GmbH, with a newly developed 3D *in silico* prediction tool.

Comparison of Manual Versus Automated Patch Clamping

In addition to developing the new *in silico* prediction algorithms, we separately used clustered hit series to develop the model against sets of compounds with limited diversity. This rationale was taken because we were seeking a tool that is capable of differentiating between the hERG channel binding potency of closely related compounds that are much less likely to be distinguished by the available 2D models. For the first hit series, we therefore tested 65 compounds in automated patch-clamp experiments, including the compounds already tested manually to corroborate the correlation between the different technologies. *Figure 2* shows that both methods correlated very well, within experimental error, for the compounds that were tested on both devices and this allowed us to broaden the basis of the electrophysiological data to be employed as a test set for the development of *in silico* prediction tools.

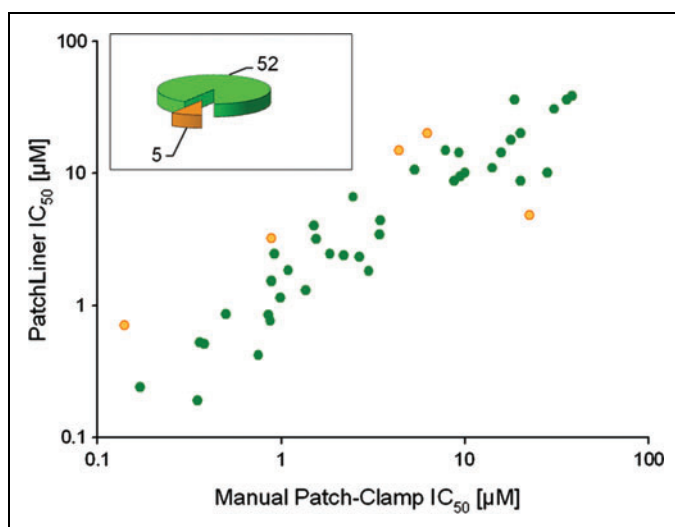


Fig. 2. Correlation between manual and automated patch-clamp data. For 52 of 57 compounds the IC_{50} values differed by a factor < 3 ; for 5 of 57 compounds the IC_{50} values differed by a factor of between 3 and 5. Color images available online at www.liebertonline.com/adt.

Three-Dimensional Quantitative Structure–Activity Relationship

The hERG channel pore is large and flexible and therefore poses a challenge for docking protocols. A number of hERG QSAR models have been described in the literature.²⁷ Without a pharmacophore-guided docking procedure, ligand docking becomes less accurate and can lead to a number of false-positive docking poses. To overcome this problem, we used our three-feature pharmacophore query to constrain the docking solutions, as implemented in MOE. Pharmacophore-based models have been designed to create generic models for hERG,³⁴ and ligand-based models have also been built using Tripos' comparative molecular field analysis, comparative molecular shape indices analysis, and the Accelrys' catalyst^{35–37} software. Our approach was to build a 3D QSAR modeling protocol derived from multivariate analysis, which could be tailored to a focused compound series. The molecular descriptors used in the QSAR model were derived from ligand-based attributes and ligand–protein interactions and from fit to the pharmacophore model described above. Ligand data sets were prepared using MOE and clustered in training and test sets following a spectral clustering algorithm using UNITY fingerprints.³⁸ The ligands were docked into the hERG homology model described earlier using MOE²⁴ with three weighted regions describing the three-feature pharmacophore spheres (labeled F1, F2, F3). The two aromatic weighted regions (F1 and F3) were 1.5 Å in radius with a weight of 5, and an atom-centered weight of 5 enveloped a radius of 1.5 Å to describe the cationic pharmacophore feature F2. Following docking, the poses were visualized in the CCDC Silver software,³⁹ from which a number of descriptors were calculated from a variety of protein–ligand interactions, including hydrogen bonds, the solvent inaccessible ligand surface area, and volume features. These

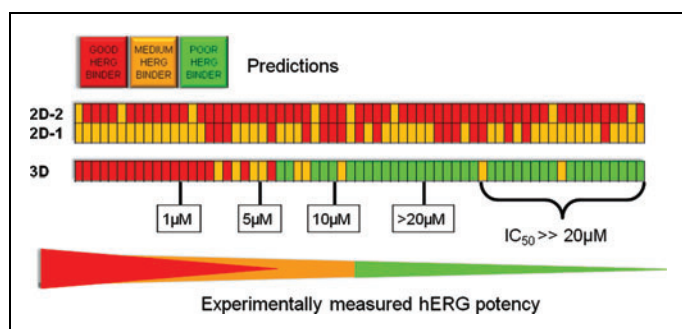


Fig. 3. Comparison of the 2D quantitative structure–activity relationship and the 3D model prediction of hERG channel blockade for a set of H3R program ligands. The two bars show the 2D predictions. All compounds are predicted to be highly or medium active by the 2D models in this set. The bottom bar is labeled with the experimentally determined hERG IC_{50} measurements and shows how the 3D model was able to separate out hERG highly actives, hERG medium-actives, and hERG low-activity/inactive. 3D, three dimensional. Color images available online at www.liebertonline.com/adt.

descriptors were added to 2D MOE QSAR descriptors, pharmacophore feature information was collated, and the statistical program SIMCA-P, version 11, was used in the generation of partial least squares models.⁴⁰ The models were validated as described in the literature.⁴¹ To prove the advantage of the 3D model over the 2D model, we subjected the test set of compounds to both the 2D and 3D *in silico* prediction tools. *Figure 3* shows that the 2D models failed to predict a ranking within the series at all, although the set of compounds comprised a broad range of IC_{50} values against hERG from 70 nM to

>20 μ M (estimated IC_{50} values above highest concentration tested). The vast majority of the compounds were predicted by the 2D models to block the hERG channel, which did not correlate with the data obtained in electrophysiology, showing that the 2D model is very limited in its predictivity and not a useful tool for a hit-to-lead campaign involving compounds where the target and hERG pharmacophores are so similar. The result was different when employing the 3D model. Here the ranking correlated well with the electrophysiology data. The most potent hERG blockers were correctly identified, and more importantly, compounds that were free of any major hERG liability in electrophysiology were predicted to be inactive or only weak hERG blockers (*Fig. 3*).

In addition to this increased predictive power, the major advantage of the 3D model is the ability to guide future chemistry in a rational manner using the integration of electrostatic interactions in the prediction, which can be visualized by areas of attraction and areas of repulsion. To illustrate this, *Figure 4* shows a pair of compounds (2a and 2d) that have a high structural similarity but differ significantly in their affinity toward the hERG channel. Both of these compounds were predicted to be mid-high-range hERG active by the two 2D hERG models. For compound design, these ESPC fields can be employed in two different ways: either by seeking to design molecules that will directly decrease the highlighted areas of attraction, or by seeking to increase the size or magnitude of areas of repulsion. Sometimes, it is possible to build repulsive groups that directly screen out the effect of attractive groups without actually moving/removing the attractive group. More specifically, for compound 2a, the F1 aromatic/acceptor region shows significant attraction to the hERG pore. Modification of the F1 group for 2d makes this group to repel hERG, even though the pharmacophoric nature of the group is sim-

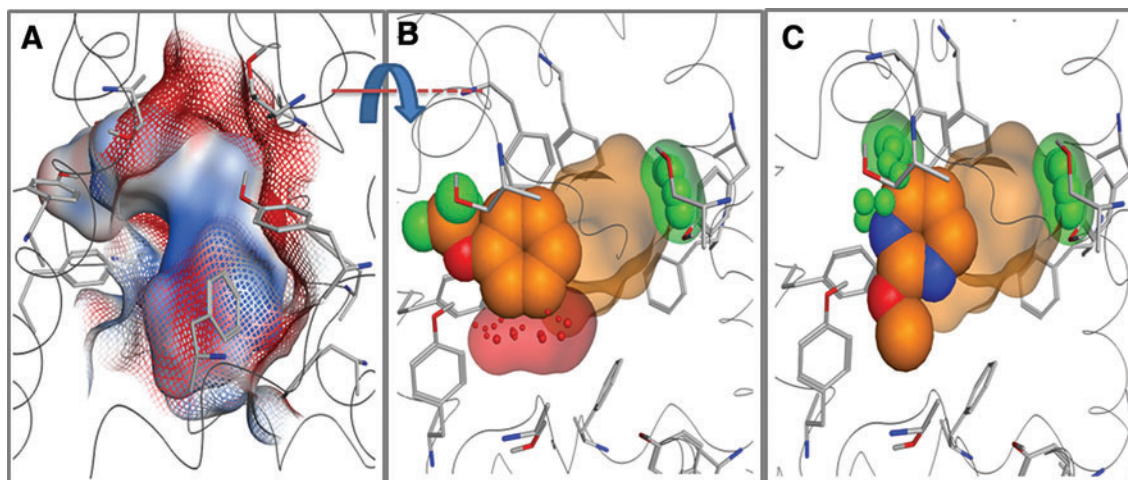


Fig. 4. (A) Electrostatic field of the internal hERG pore overlaid on the electrostatic surface of the docked compound **2a**. These two electrostatic fields are translated into an EC field for the two. (B) “Hot spots” of attraction (red) and repulsion (green) can then be observed within this EC field, as seen for **2a** in B, where the F1 aromatic/acceptor region shows significant attraction to the hERG pore. (C) Modifying the F1 group for **2d** so that it repels hERG, even though the pharmacophoric nature of the group is similar, shows the ability of EC to guide abolition of hERG activity. Panels B and C are rotated 90° relative to A in order to better observe the modified EC. EC, electrostatic complementarity.

ilar. This shows the ability of electrostatic complementarity to guide abolition of hERG activity through relatively minor structural changes.

Impact on Compound Design

The 3D hERG homology model was employed during the hit-to-lead phase to identify regions of H3R antagonists where minor structural modifications, including modulating localized electrostatics, might ablate hERG blockade. Areas of electrostatic attraction and repulsion to the hERG channel, projected onto the small-molecule surfaces, directed the chemistry team to focus compound design ideas on the right-hand-side R-group (Table 2, compounds 2a–2d). As the effective changes were solely made in the diversity region, we do not reveal the scaffold because that does not add any crucial information to the presented investigation. Novel compound ideas were prefiltered

by interrogation of the 3D hERG homology model, which enabled the medicinal chemistry team to focus synthesis on structures predicted to be poor ligands for the hERG channel. Introduction of repulsive electrostatic potential in the R group region, as illustrated by 2d, removed the hERG blockade (MPC hERG $IC_{50} > 20,000$ nM) while retaining low single-digit nanomolar human H3R potency. The predictive power of the 3D hERG model is further exemplified through successful identification of 2c as hERG active, whereas the close structural homolog 2d was predicted to be inactive at hERG.

Implementation of the 3D hERG model during the H2L compound design led to a significant reduction (41% down to 10%) in synthesized hERG-active H3R antagonists. The percentage of synthesized compounds with reduced risk of hERG blockade while retaining significant H3R antagonism ($IC_{50} < 100$ nM) was also improved from 59% to 88% after integration of the novel docking procedures. If one plots the potency to block the hERG channel in the order of the synthesis of the molecules as depicted in Figure 5, it becomes apparent that the used approach helped to reduce the number of compounds with hERG liability ($pIC_{50} > 4.7$).

As H3R and hERG channel binders share essential pharmacophore points, only small modifications are allowed in order to abolish hERG affinity but still maintain target activity. The 3D model, involving docking, 3D QSAR, and finally ESPC, vastly increases the ability to accurately rank hERG actives versus 2D QSAR models for closely related compounds. It has been known that the hERG channel affinity is very sensitive to small structural changes to the compound.²⁷ We wanted to use this phenomenon to reduce hERG affinity but required a method to reveal these “hot spots” of possible molecular change. The purpose of calculating the electrostatic complementarity between a ligand and the hERG channel is to assist in recognition of the “hot spots,” which are therefore represented in the form of electrostatic repulsion or attraction. And indeed, we have found that these areas appear to be highly sensitive to small structural changes to the compound.


The availability of medium-throughput electrophysiology technologies has enabled us to establish and validate the *in silico* prediction tools in a manner that would not have been possible if we had solely to rely on MPC devices.

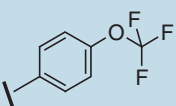
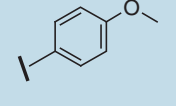
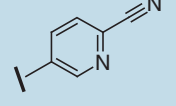
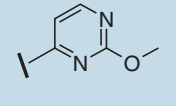
One has to take into account that the stimulation protocol employed is an important factor for assessing blockade of hERG activity, as different protocols may lead to different pharmacological behavior of compounds (e.g.,⁴²). The MPC protocol used in the present study has been validated with reference compounds earlier⁴³ and shown to yield IC_{50} values comparable to literature data. Additional validation of the MPC protocol and the protocol used on the PatchLiner are provided in Supplementary Table S2.

Although we show here an example of hERG profiling, we are certain that these technologies will be helpful also for other programs and for other ion channel targets of interest.

In our program, the incorporation of the hERG modeling information with knowledge of the H3R pharmacophore enabled the rapid optimization of novel H3R antagonists with low risk of undesirable hERG blockage.

Table 2. Human Histamine H3 Receptor and Human Ether- α -Go-Go-Related Gene K^+ Channel Activities of Compounds 2a–d



Compound	R	Human H3R IC_{50} (nM) ^a	hERG IC_{50} (nM)
2a		0.6	70
2b		1.3	2,670
2c		3.1	880
2d		1.7	>20,000

See Ref. 33 for complete details of human H3R assay conditions.

^aValues are arithmetic means of two or more experiments; individual values do not differ more than threefold from the mean.

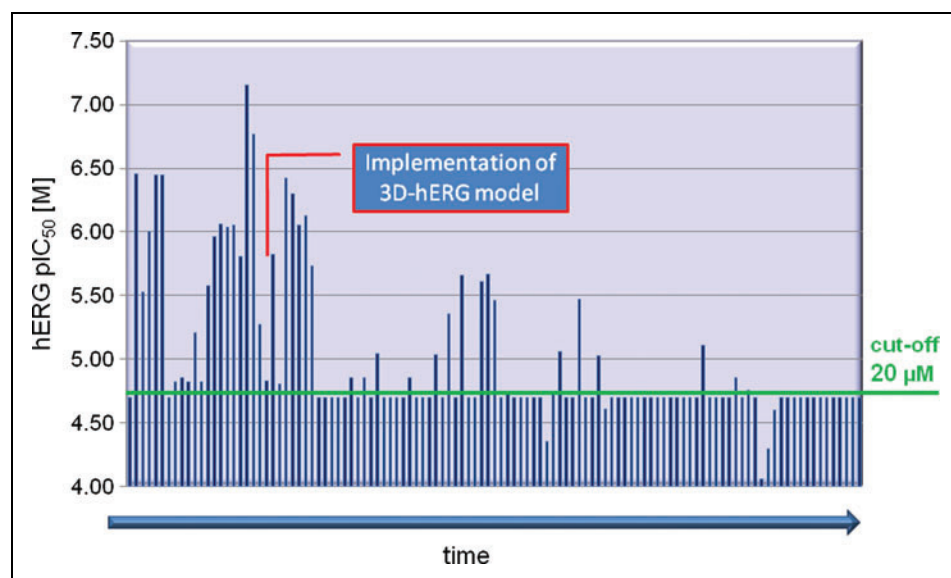


Fig. 5. hERG pIC_{50} values of project compounds depicted in synthesis chronology. The routine cutoff was set at $20\ \mu\text{M}$ in accordance with the highest concentrations tested. Selected compounds were evaluated up to $100\ \mu\text{M}$, and the resulting pIC_{50} values are included. The time point when the 3D hERG model was implemented into the compound design process is highlighted. Color images available online at www.liebertonline.com/adt.

It should be noted that the reduction of *in vitro* hERG liabilities is only a single step in developing and optimizing drug candidates and that the final conclusion whether a molecule is suitable for development depends on the overall properties, such as absorption, pharmacokinetics, free plasma ratio, and the separation between effective dose and doses resulting in adverse events.

DISCLOSURE STATEMENT

All authors are employees of Evotec.

REFERENCES

- Arrang JM, Garbarg M, Schwartz JC: Auto-inhibition of brain histamine-release mediated by a novel class (H-3) of histamine-receptor. *Nature* 1983; 302:832–837.
- Schlicker E, et al.: Histamine H3 receptor-mediated inhibition of serotonin release in the rat brain cortex. *Naunyn Schmiedebergs Arch Pharmacol* 1988; 337:588–590.
- Schlicker E, et al.: Inhibition of noradrenaline release in the rat brain cortex via presynaptic H3 receptors. *Naunyn Schmiedebergs Arch Pharmacol* 1989;340: 633–638.
- Schlicker E, et al.: Histamine inhibits dopamine release in the mouse striatum via presynaptic H3 receptors. *J Neural Transm Gen Sect* 1993;93:1–10.
- Clapham J, Kilpatrick GJ: Histamine H3 receptors modulate the release of [3H]-acetylcholine from slices of rat entorhinal cortex: evidence of the possible existence for H3 receptor subtypes. *Br J Pharmacol* 1992;107:919–923.
- Drutel G, et al.: Identification of rat H-3 receptor isoforms with different brain expression and signaling properties. *Mol Pharmacol* 2001;59:1–8.
- Martinezmir MI, et al.: Histamine receptor-H1, receptor-H2 and receptor-H3 visualized in the brain of human and nonhuman-primates. *Brain Res* 1990; 526:322–327.
- Cannon KE, et al.: Immunohistochemical localization of histamine H-3 receptors in rodent skin, dorsal root ganglia, superior cervical ganglia, and spinal cord: potential antinociceptive targets. *Pain* 2007;129:76–92.
- Gemkow MJ, Davenport AJ, Harich S, Ellenbroek BA, Cesura A, Hallett D: The histamine H3 receptor as a therapeutic drug target for CNS disorders. *Drug Dis Today* 2009;14:509–515.
- Ali SM, et al.: Design, synthesis, and structure-activity relationships of acetylene-based histamine H-3 receptor antagonists. *J Med Chem* 1999;42:903–909.
- Celanire S, et al.: Histamine H-3 receptor antagonists reach out for the clinic. *Drug Dis Today* 2005;10:1613–1627.
- Wijtmans M, Leurs R, de Esch I: Histamine H-3 receptor ligands break ground in a remarkable plethora of therapeutic areas. *Expert Opin Investig Drugs* 2007;16.7:967–985.
- Cowart M, et al.: Medicinal chemistry and biological properties of non-imidazole histamine H-3 antagonists. *Mini Rev Med Chem* 2004;4: 979–992.
- Sun MH, et al.: Synthesis and SAR of 5-amino- and 5-(aminomethyl)benzofuran histamine H-3 receptor antagonists with improved potency. *J Med Chem* 2005;48:6482–6490.
- Zhao C, et al.: The alkaloid conessine and analogues as potent histamine H-3 receptor antagonists. *J Med Chem* 2008;51:5423–5430.
- Nagase T, et al.: Synthesis, structure-activity relationships, and biological profiles of a quinazolinone class of histamine H-3 receptor inverse agonists. *J Med Chem* 2008;51:4780–4789.
- Lau JF, et al.: Ureas with histamine H-3-antagonist receptor activity—a new scaffold discovered by lead-hopping from cinnamic acid amides. *Bioorg Med Chem Lett* 2006;16:5303–5308.
- Hancock AA: The challenge of drug discovery of a GPCR target: analysis of preclinical pharmacology of histamine H-3 antagonists/inverse agonists. *Biochem Pharmacol* 2006;71:1103–1113.
- Roche O, Sarmiento RMR: A new class of histamine H-3 receptor antagonists derived from ligand based design. *Bioorg Med Chem Lett* 2007;17:3670–3675.
- Lazewska D, et al.: Piperidine variations in search for non-imidazole histamine H3 receptor ligands. *Bioorg Med Chem* 2008;16:8729–8736.
- Sander K, von Coburg Y, Camelin J-C, Ligneau X, Rau O, Schubert-Zsilavecz M, Schwartz J-C, Stark H: Acidic elements in histamine H3 receptor antagonists. *Bioorg Med Chem Lett* 2010;20:1581–1584.
- Aronov AM: Predictive *in silico* modeling for hERG channel blockers. *Drug Dis Today* 2005;10:149–155.
- Seierstad M, Agrafiotis DK: A QSAR model of hERG binding using a large, diverse, and internally consistent training set. *Chem Biol Drug Des* 2006;67:284–296.
- [MOE] The Molecular Operating Environment: Version 2009.10, software available from Chemical Computing Group Inc., 1010 Sherbrooke Street West, Suite 910, Montreal, Canada H3A 2R7. www.chemcomp.com.
- Farid R, et al.: New insights about HERG blockade obtained from protein modeling, potential energy mapping, and docking studies. *Bioorg Med Chem* 2006;14:3160–3173.
- Aronov AM, Goldman BB: A model for identifying HERG K+ channel blockers. *Bioorg Med Chem* 2004;12:2307–2315.
- Diller DJ: *In silico* hERG modeling: challenges and progress. *Curr Comput Aided Drug Des* 2009;5:106–121.

28. Chau R-L, Dean RM: Electrostatic complementarity between proteins and ligands. Charge disposition, dielectric and interface effects. *J Comput Aided Mol Des* 1994;8:513-525.
29. Heifetz A, Katchalski-Katzir E, Eisenstein M: electrostatics in protein-protein docking. *Protein Sci* 2002;11:571-587.
30. Grant JA, Pickup BT, Nicholls A: A smooth permittivity function for poisson-boltzmann solvation methods. *J Comput Chem* 2001;22:608-640.
31. Nicholls A, Grant JA: Molecular shape and electrostatics in the encoding of relevant chemical information. *J Comput Aided Mol Des* 2005;19:661-686.
32. Hamill OP, Marty A, Neher E, Sakmann B, Sigworth FJ: Improved patch-clamp techniques for high-resolution current recording from cells and cell-free membrane patches. *Pflugers Arch* 1981;391:85-100.
33. Davenport AJ, Hallett DJ, Corsi M: Azetidines and cyclobutanes as Histamine H3 Receptor Antagonists. WO/2009/135842.
34. Aronov AM, Goldman BB: A model for identifying HERG K⁺ channel blockers. *Bioorg Med Chem* 2004;12:2307-2315.
35. Pearlstein RA, Vaz RJ, Kang J, Chen X-L, Preobrazhenskaya M, Shchekotikhin AE, Korolev AM, Lysenkova LN, Miroshnikova OV, Hendrix J, Rampe D: Characterization of HERG potassium channel inhibition using CoMSIA 3D QSAR and homology modeling approaches. *Bioorg Med Chem Lett* 2003;13:1829-1835.
36. Ekins S, Crumb WJ, Sarazan RD, Wikel JH, Wrighton SA: Three-dimensional quantitative structure-activity relationship for inhibition of human *Ether-a-Go-Go*-related gene potassium channel. *JPET* 2002;301:427-434.
37. Cavalli A, Poluzzi E, De Ponti F, Recanatini M: Toward a pharmacophore for drugs inducing the long QT syndrome: insights from a CoMFA study of HERG K⁺ channel blockers. *J Med Chem* 2002;45:3844-3853.
38. Brewer M: Development of a spectral clustering method for the analysis of molecular data sets. *J Chem Inf Model* 2007;47:1727-1733.
39. CCDC (2005). SILVER-A program for the post-processing of GOLD docking results. Cambridge Crystallographic Data Centre, 12 Union Road, Cambridge, England.
40. SIMCA-P, 11.0.0.0: Umetrics AB, Umeå, Sweden, 2005. www.umetrics.com/simca.
41. Mazanetz MP, Withers IM, Laughton CA, Fischer PM: *QSAR Comb Sci* 2009; 28:878-884.
42. Milnes JT, Witchel HJ, Leaney JL, Leishman DJ, Hancox JC: Investigating dynamic protocol-dependence of hERG potassium channel inhibition at 37 degrees C: Cisapride versus dofetilide. *J Pharmacol Toxicol Methods* 2010;61:178-191.
43. Deisemann H, Ahrens N, Schlobohm I, Kirchoff C, Netzer R, Möller C: Effects of common antitussive drugs on the hERG potassium channel current. *J Cardiovasc Pharmacol* 2008;52:494-499.

Address correspondence to:

Dr. Mark J. Gemkow

Evotec AG

Schnackenburgallee 114

22525 Hamburg

Germany

E-mail: mark.gemkow@evotec.com